

Supplementary Material

Bioactivity Profiles on 15 Different Effect Mechanisms for 15 Golden Root Products via High-Performance Thin-Layer Chromatography, Planar Assays, and High-Resolution Mass Spectrometry

Hanna Nikolaichuk ¹⁻³, Irena M. Choma ² and Gertrud E. Morlock ^{1,*}

¹ Chair of Food Science, Institute of Nutritional Science, Justus Liebig University Giessen,

Heinrich-Buff-Ring 26-32, 35392 Giessen, Germany

² Department of Chromatography, Faculty of Chemistry, Maria Curie-Skłodowska University

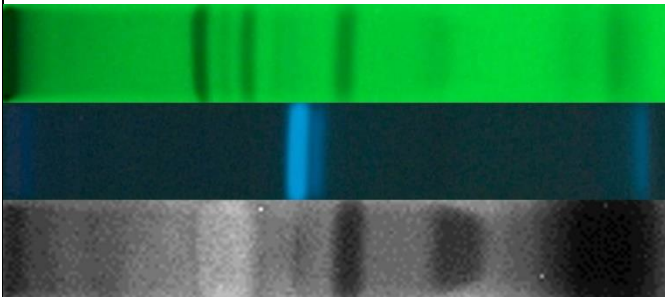
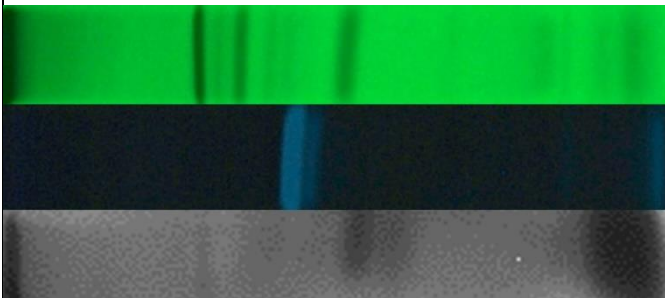
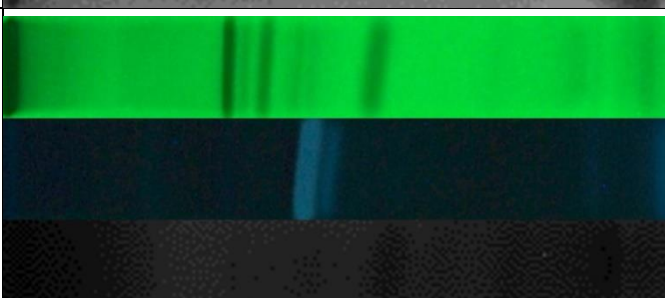

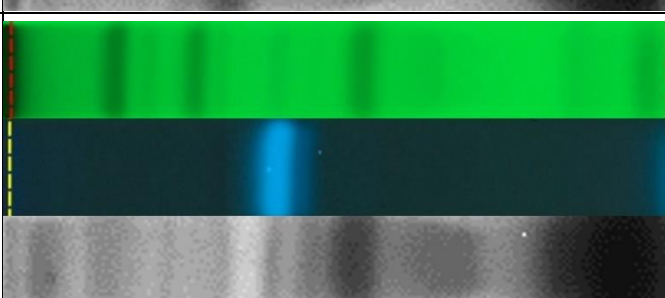
Maria Curie-Skłodowska sq.3, 20031 Lublin, Poland

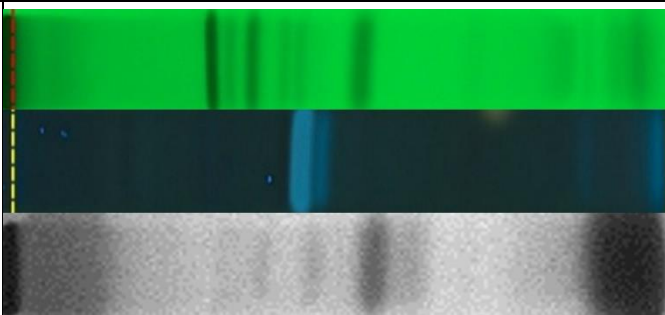
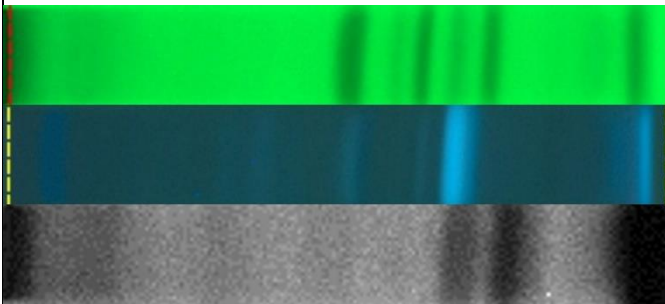
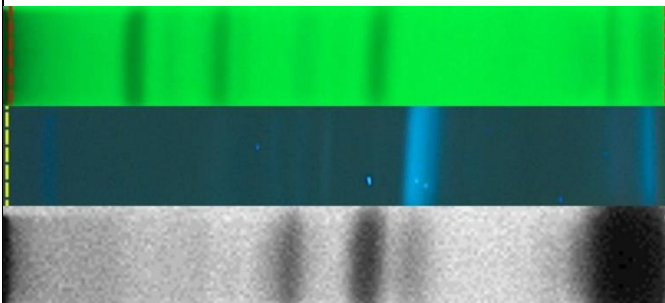
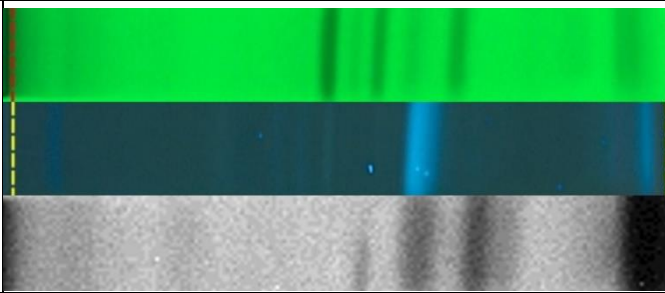
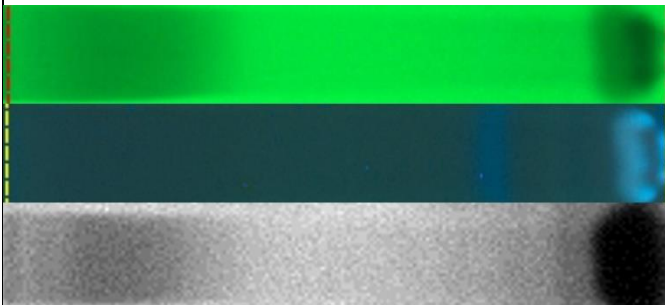
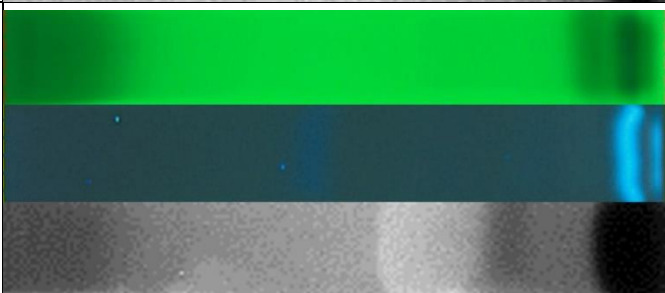
³ Department of Bioanalytics, Faculty of Biomedicine, Medical University of Lublin,


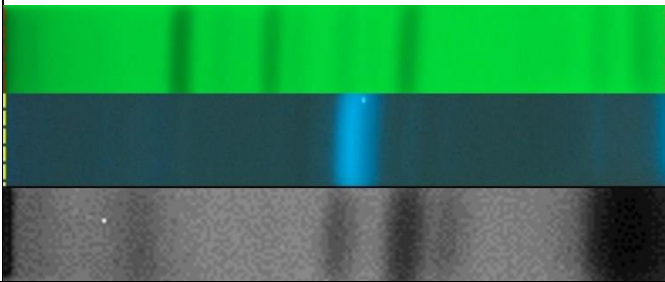
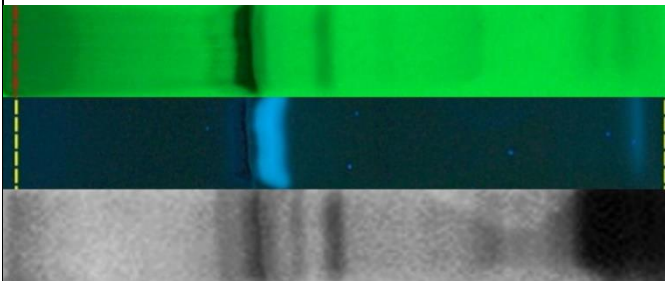
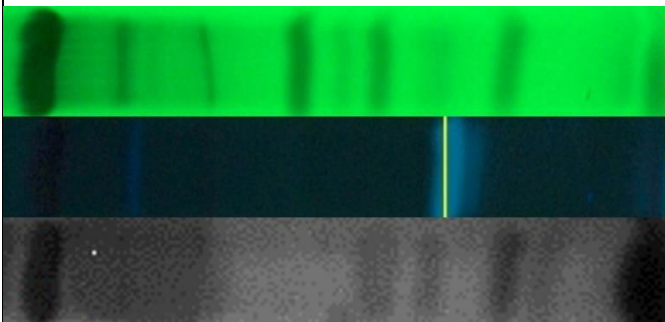
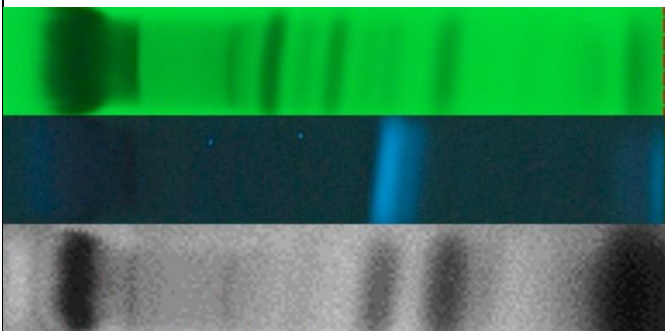
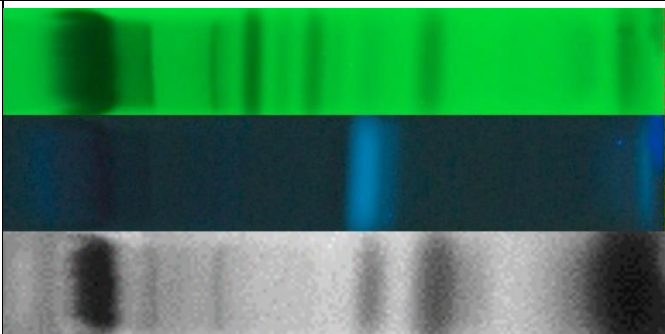
Jaczewskiego st. 8b, 20090, Lublin, Poland

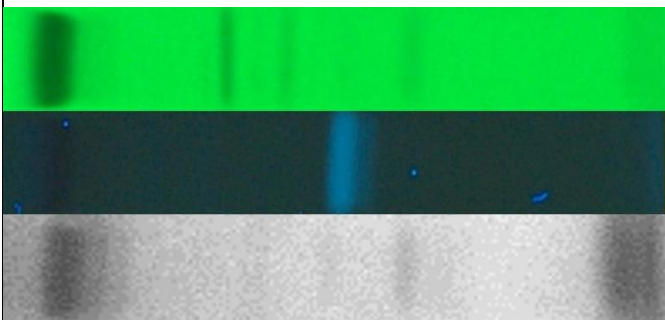
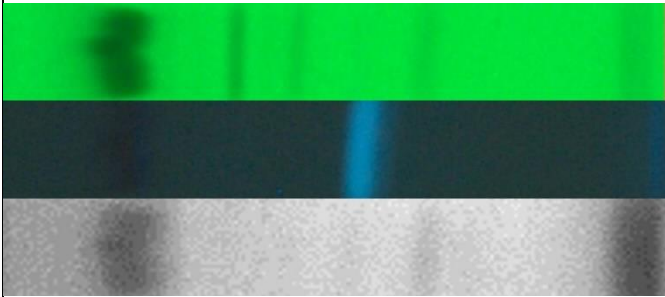
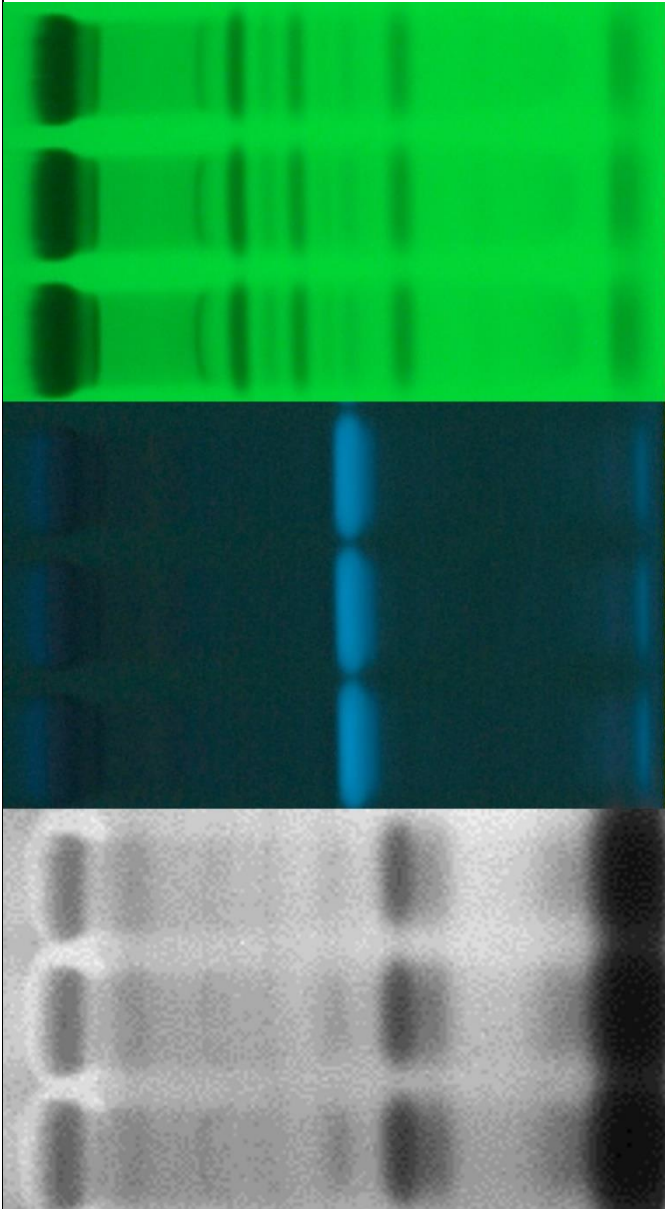
* Correspondence: Gertrud.Morlock@ernaehrung.uni-giessen.de

Table S1 Mobile phase optimization for a golden root extract (5 µL/band or 3–4 µL/band) separated on the HPTLC plate silica gel 60 F₂₅₄ with the specified mobile phase system

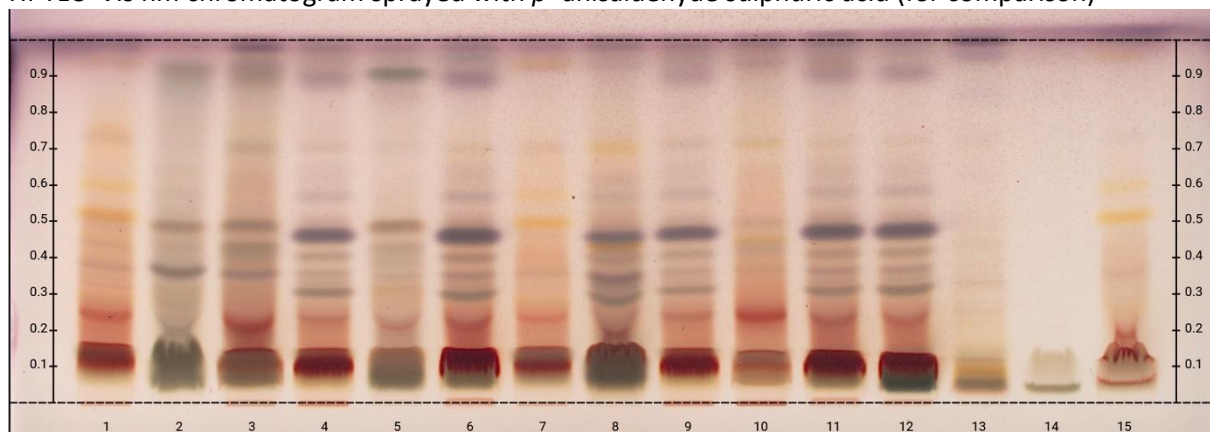
MP	Solvent composition	Ratio (V/V)	Chromatogram at 254 nm, FLD 366 nm and bioluminescence after <i>Aliivibrio fischeri</i> bioassay
1	Ethyl acetate-methanol-water	7.7:1.3:1	
2	Ethyl acetate-methanol-water-acetic acid	7.7:1.3:1:0.1	
3	Ethyl acetate-methanol-water-acetic acid	7.7:1.3:1:0.2	
4	Ethyl acetate-acetonitrile-water	7:2:1	
5	Ethyl acetate-acetonitrile-water	5:4:1	

6	Ethyl acetate-methanol-water-acetic acid	7.7:1.3:1:0.15	
7	Ethyl acetate-methanol-water-acetic acid	7:1.5:1:0.2	
8	Ethyl acetate-acetonitrile-water-acetic acid	5:4:1:0.1	
9	Ethyl acetate-methanol-water-acetic acid	7:1.5:1:0.1	
10	Ethyl acetate-methanol-water-acetic acid	5:4:1:0.1	
11	Ethyl acetate-methanol-water-acetic acid	6:3:1:0.1	

12	Ethyl acetate-methanol- water-acetic acid	7:2:1:0.1	
13	Ethyl acetate-acetonitrile- water-acetic acid	4:5:1:0.1	
14	Focusing (methanol), 3 cm Ethyl acetate-water	10:1	
15	Focusing (acetone, 2 x methanol), 2 cm Ethyl acetate-methanol- water-acetic acid	7:1.5:1.5:0.1	
16	Ethyl acetate-methanol- water-acetic acid	7:1.5:1.5:0.1	
17	Focusing (2 x acetone, methanol), 2 cm Ethyl acetate-methanol- water-acetic acid	7:1.5:1.5:0.1	

18	Ethyl acetate-methanol- water-acetic acid	7:1.5:1.5:0.1	
19	Focusing (2 x acetone, methanol), 2 cm Ethyl acetate-methanol- water-acetic acid	7:1.5:1.5:0.1	
20	Ethyl acetate-methanol- water-acetic acid	7:1.5:1.5:0.1	

HPTLC–Vis nm chromatogram sprayed with *p*-anisaldehyde sulphuric acid (for comparison)



HPTLC–FLD 366 nm chromatogram sprayed with *p*-anisaldehyde sulphuric acid (for comparison)

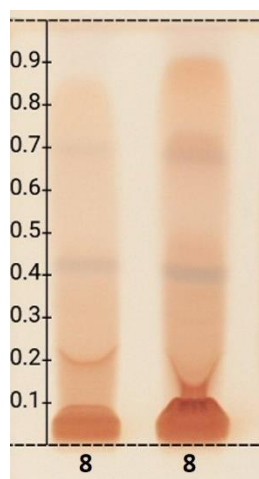
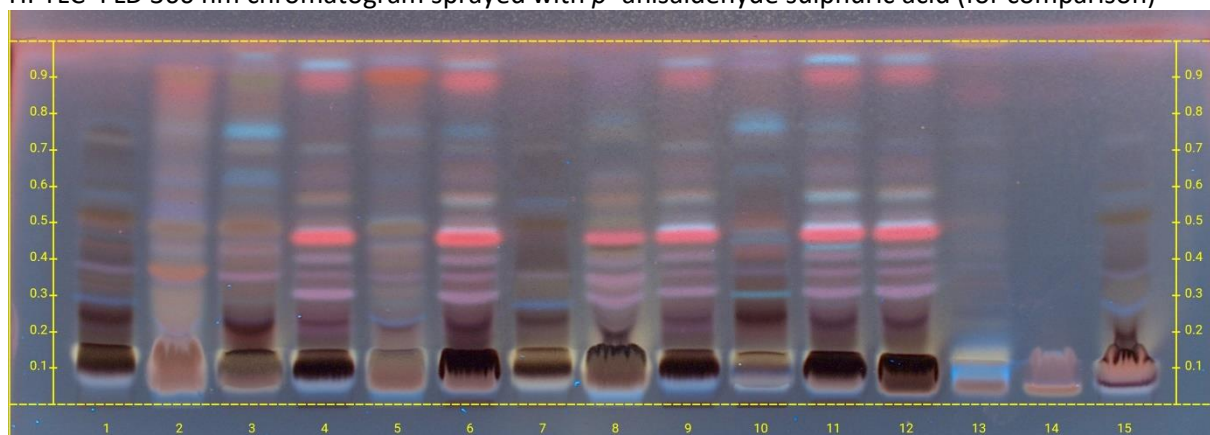


Figure S1. HPTLC–Vis chromatogram after derivatization via Fast Blue B salt reagent (0.5% aqueous solution) of a golden root extract ID 8 (200 and 400 µg/band) separated on HPTLC plate silica gel 60 F₂₅₄ with ethyl acetate-methanol-water-acetic acid 70:15:15:1 (V/V/V/V) [GM1] and detected at white light illumination.

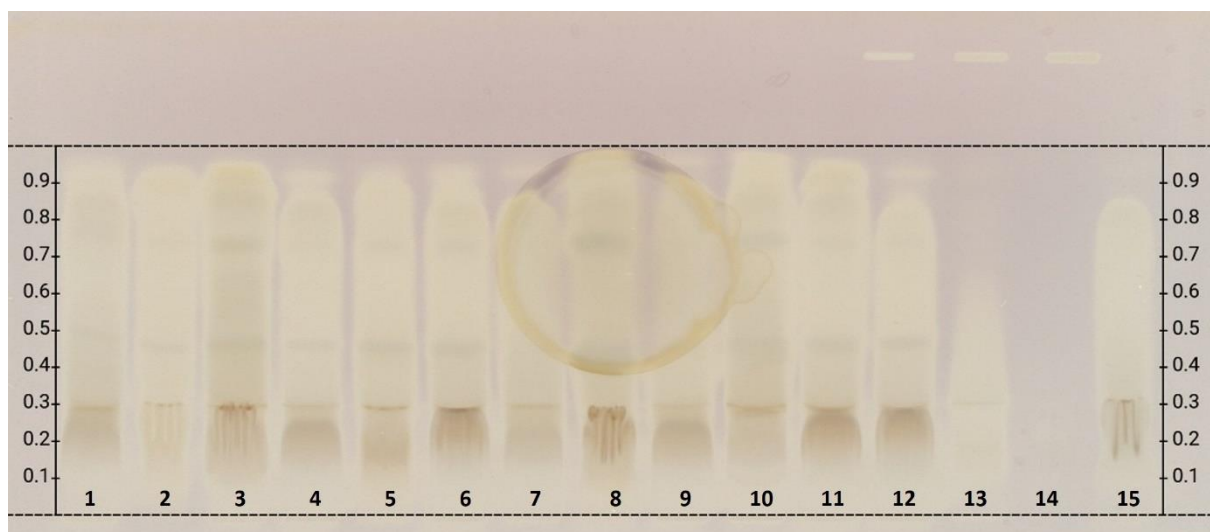
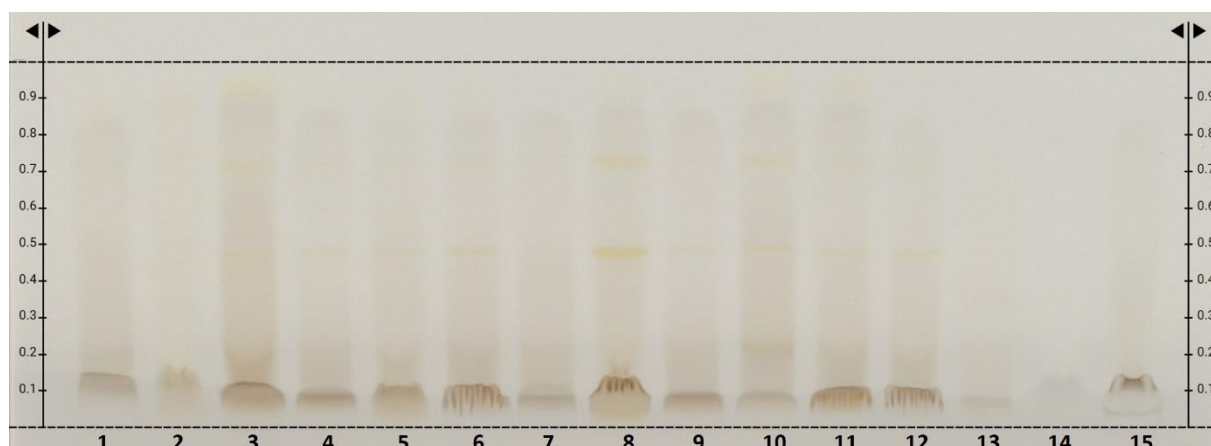
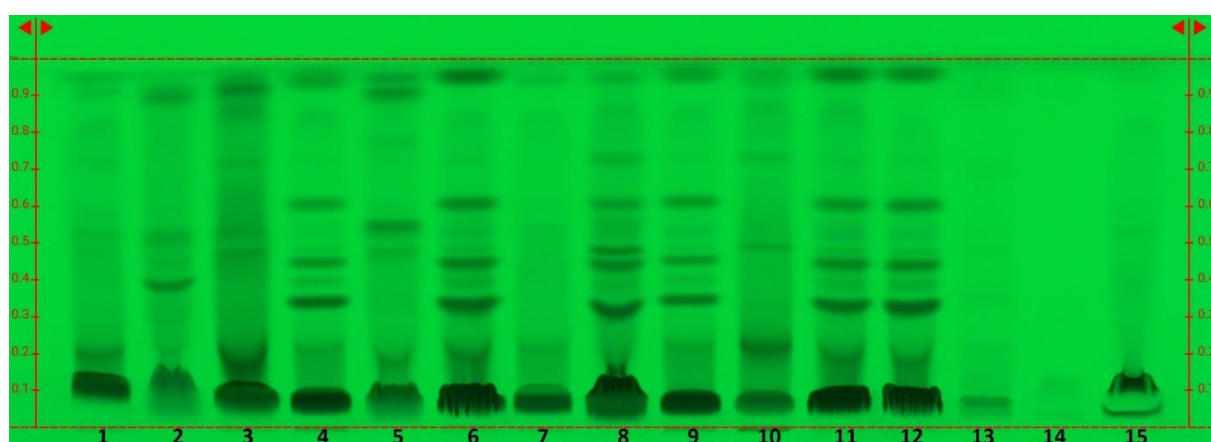


Figure S2. DPPH•–Vis autogram of golden root extract IDs 1–15 (400 µg/band each) separated on HPTLC plate silica gel 60 F₂₅₄ with ethyl acetate-methanol-water-acetic acid 70:15:15:1 (V/V/V/V) and detected at white light illumination after the DPPH• assay. Positive control gallic acid in the right upper plate corner. The ring in the plate middle was caused by malfunction of the Derivatizer nozzle.

HPTLC–Vis nm chromatogram (for comparison)



HPTLC–UV 254 nm chromatogram (for comparison)



HPTLC–FLD 366 nm chromatogram (for comparison)

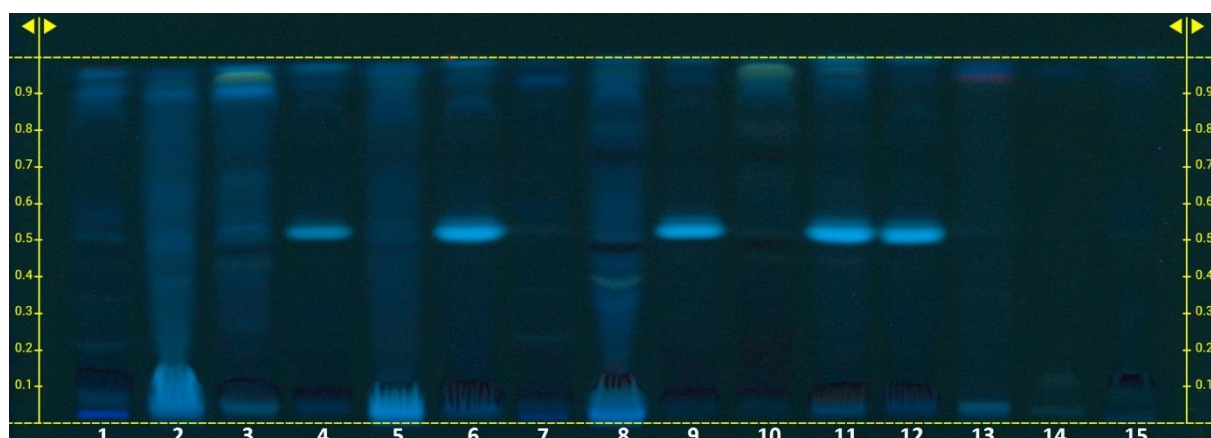
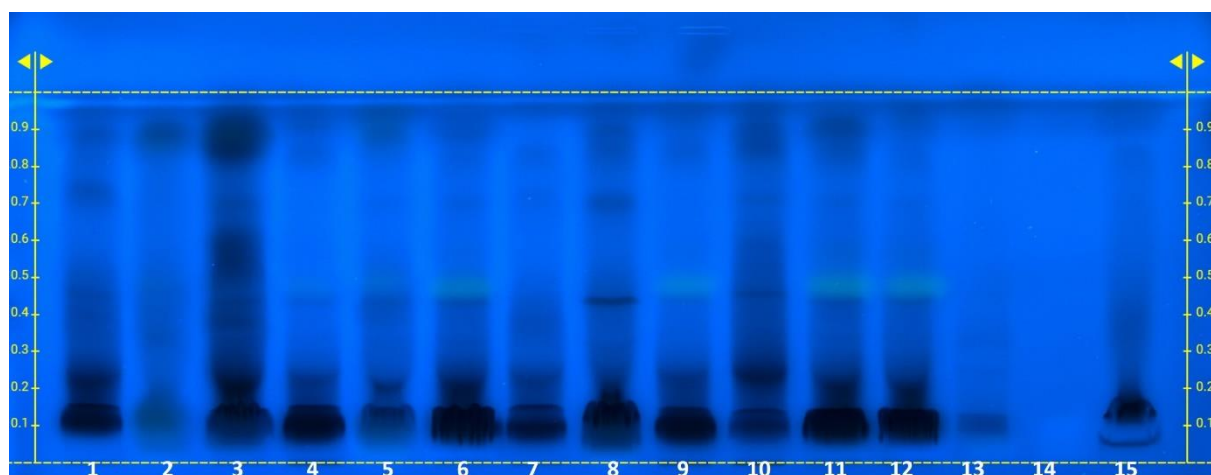
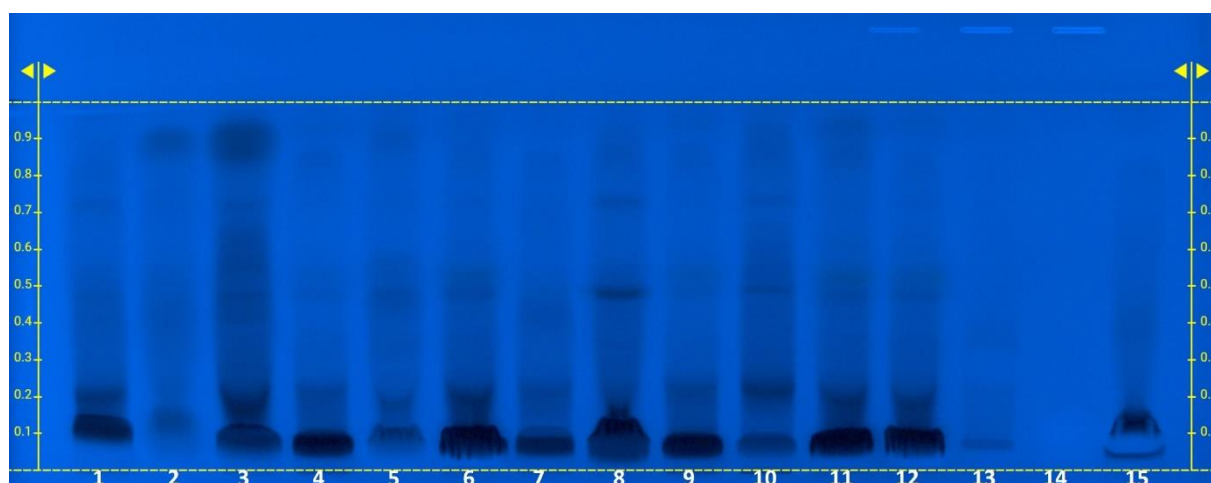


Figure S3. HPTLC– α/β -glucosidase inhibition autograms at FLD 366 nm in comparison to HPTLC–Vis/UV/FLD chromatograms of golden root extracts IDs 1–15 (400 $\mu\text{g}/\text{band}$ each) separated on HPTLC plate silica gel 60 F_{254} with ethyl acetate-methanol-water-acetic acid 70:15:15:1 (V/V/V/V) and detected at FLD 366 nm after the respective glucosidase assay *versus* only sprayed with 4-methylumbelliferone solution. The positive controls (applied at plate top as ethanolic solution) were acarbose (3, 9, and 18 $\mu\text{g}/\text{band}$) and imidazole (2, 5, and 8 $\mu\text{g}/\text{band}$) for the α/β -glucosidase, respectively.

HPTLC- α -glucosidase inhibition autogram at FLD 366 nm



HPTLC- β -glucosidase inhibition autogram at FLD 366 nm



HPTLC-FLD 366 nm chromatogram sprayed with 4-methylumbelliferone solution

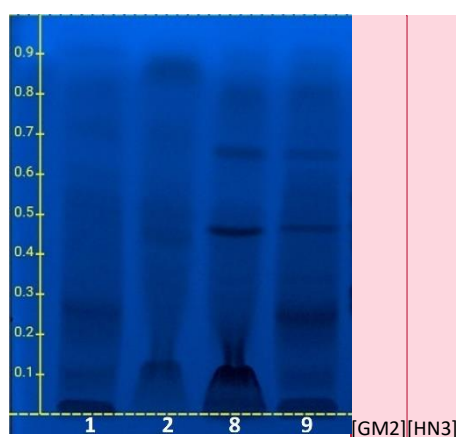


Figure S3. Continued.

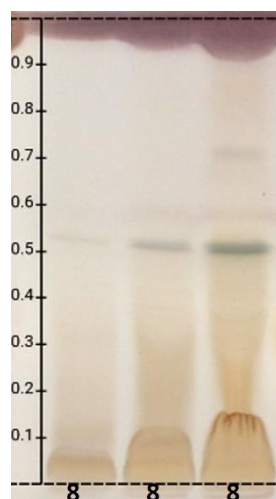
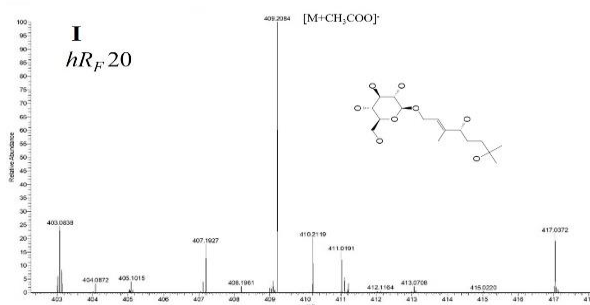
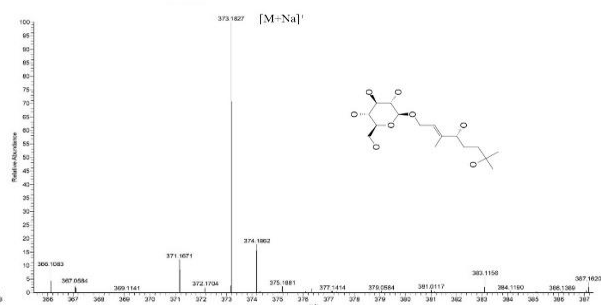


Figure S4. HPTLC- α -amylase inhibition autogram of golden root extract ID 8 (100, 200 and 400 $\mu\text{g}/\text{band}$) separated on HPTLC plate silica gel 60 F_{254} with ethyl acetate-methanol-water-acetic acid (70:15:15:1, V/V/V/V) and detected at white light illumination after the α -amylase inhibition assay.

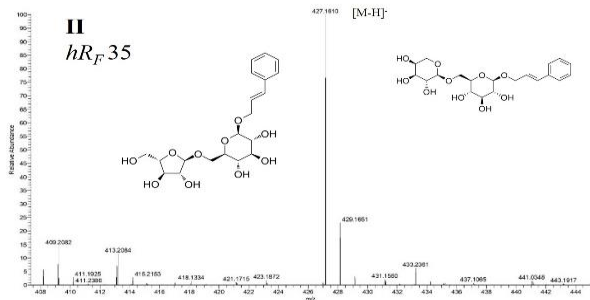
HRMS negative mode



HRMS positive mode



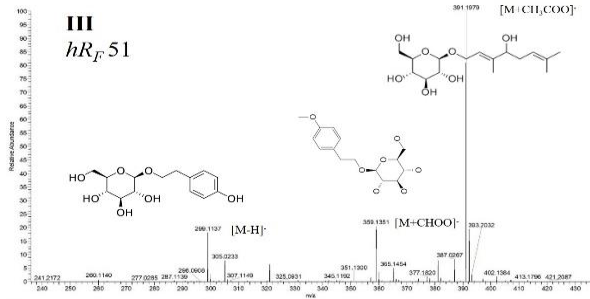
II



Mass spectrum of compound 10. The x-axis represents the mass-to-charge ratio (m/z) from 400 to 500, and the y-axis represents relative intensity from 0 to 100. The base peak is at m/z 451.1579, corresponding to the $[M+Na]^+$ ion. Other labeled peaks include m/z 469.2047, 481.1884, and 483.2155. The chemical structure of compound 10 is shown above the spectrum.

III

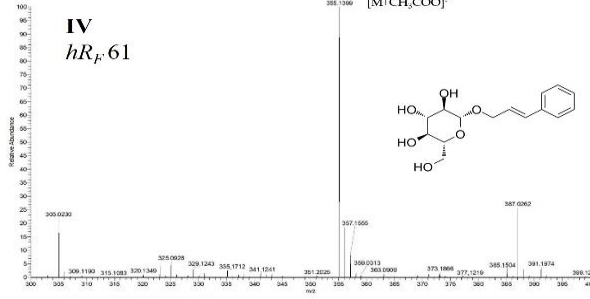
$hR_F 51$



Mass spectrum of compound 10. The x-axis represents the mass-to-charge ratio (m/z) from 305 to 375. The y-axis represents the relative intensity from 0 to 100. The base peak is at m/z 365.1253, labeled $[M+Na]^+$. Other significant peaks are at m/z 337.1261, labeled $[M+Na]^+$, and m/z 353.1568. The chemical structure of compound 10 is shown above the spectrum.

CC(C)/C=C/C(O)C1OC(OC2=CC=CC=C2CO3OC(=O)OC(=O)O3)C(O)C1O

IV
hR_F 61



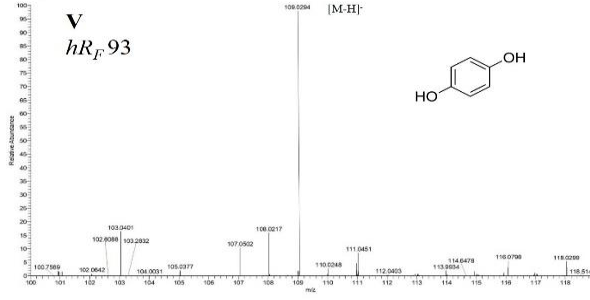
Mass spectrum of compound 10. The x-axis represents the mass-to-charge ratio (m/z) from 222 to 420, and the y-axis represents the relative intensity from 0 to 100. The base peak is at m/z 319.1148. The chemical structure of compound 10 is shown as an inset.

Chemical structure of compound 10: O[C@H]1O[C@@H](O[C@H]2[C@H](O)[C@@H](O)[C@H](O)[C@H]2O)[C@H](O)[C@H](O)[C@H]1O (a substituted sugar derivative).

Mass spectrum data (approximate relative intensity):

m/z	Relative Intensity (%)
226.0877	1
241.0929	10
254.0823	1
263.0735	1
277.0691	1
283.0746	1
293.0693	1
302.1747	1
313.1793	1
319.1148	100
322.1334	1
327.0816	1
341.0906	1
351.0908	10
355.1720	1
367.0903	1
376.3175	1
401.1178	1
408.0907	1
418.0900	1

V
hR_F 93



Mass spectrum of $[M-H]^-$ showing relative intensity versus m/z . The base peak is at m/z 113.0444. Other significant peaks are labeled at m/z 102.0904, 104.1074, 105.0960, 106.0886, 109.0651, 115.0577, 116.0369, 116.0903, 117.0918, 118.0062, and 120.0574. The chemical structure of 4-hydroxyphenol is shown.

VI

$hR_F 23$

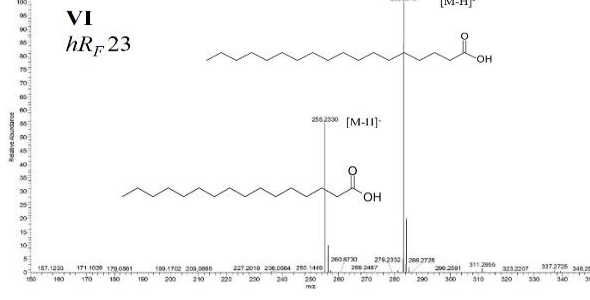


Figure S5. HPTLC–HPLC–HESI–HRMS spectra of selected bioactive zones